Tectonic and geochronological implications of variably timed magnetizations carried by authigenic greigite in marine sediments from New Zealand

Christopher J. Rowan*
Andrew P. Roberts
Southampton Oceanography Centre, European Way, Southampton SO14 3ZH, UK

ABSTRACT

Detailed scanning electron microscope observations, coupled with elemental microanalysis, confirm the presence of a chemical remanent magnetization carried by authigenic greigite (Fe_3S_4) in uplifted Neogene marine sediments from the Hikurangi Margin of New Zealand. Normal polarity samples from the studied section have declinations that are deflected ~60° clockwise of reversed polarity samples, indicating the presence of two distinct magnetizations separated by several million years of tectonic rotation about a vertical axis. However, although multiple generations of iron sulfide growth are observed petrographically, we see no clear differences in the relative timing of greigite formation between samples carrying these two magnetizations. Not only can the diagenetic growth of greigite in fine-grained marine sediments occur long after deposition, obscuring tectonic and magnetostratigraphic information, but such remagnetizations are also difficult to distinguish from a more primary signal in the absence of constraints from field tests. Our observations emphasize that considerable care is necessary when interpreting paleomagnetic data from greigite-bearing sediments.

Keywords: greigite, remagnetization, New Zealand, tectonics, magnetostratigraphy.

INTRODUCTION

The ferrimagnetic iron sulfide greigite (Fe_3S_4) is being increasingly reported as a carrier of remanent magnetizations in marine sediments (Roberts and Weaver, 2005, and references therein). Greigite is an authigenic mineral that forms as a metastable precursor to framboidal pyrite (Wilkin and Barnes, 1997). Pyritization occurs in anoxic sedimentary environments in the presence of dissolved iron and sulfide (H_2S, HS^-) released by sulfate reduction during the microbial degradation of organic matter (Berner, 1984). When reactive iron is abundant and dissolved sulfide concentrations are low, pyritization can be arrested and greigite can be preserved (Kao et al., 2004), creating a chemical remanent magnetization (CRM). In many environments, anoxic conditions can exist only a few millimeters below the sediment-water interface, allowing greigite to form soon after deposition and to preserve a syndepositional paleomagnetic signal. However, this is not necessarily the case; recent studies have identified inconsistent polarity records (e.g., Florindo and Sagnotti, 1995; Roberts and Weaver, 2005; Sagnotti el al., 2005) and even contradictory polarities within the same horizon (e.g., Jiang et al., 2001) that demonstrate late diagenetic growth of greigite.

We identify here two distinct CRMs carried by greigite, in tectonically uplifted Neogene marine sediments from the Hikurangi Margin, North Island, New Zealand. Parts of this region have undergone as much as 90° of tectonic rotation about a vertical axis during the Neogene (Rait et al., 1991). Paleomagnetic data have been extensively used to constrain the location, rates, and timings of these rotations (Walcott, 1989), and are crucial in linking past deformation to the contemporary vertical-axis rotations revealed by geodetic studies (Beavan and Haines, 2001). In addition, thick successions in this region, dated by magnetostratigraphy, provide standard midlatitude sections for foraminiferal biostratigraphy. To assure the reliability of such studies, the identification of late-forming CRMs in these sediments is essential. At the locality studied here, paleomagnetic analysis reveals a patchy development of the later CRM, with a much earlier remanence still preserved in parts of the outcrop. This provides an excellent opportunity to examine the petrographic differences resulting from differently timed magnetizations. We have undertaken detailed scanning electron microscope (SEM) observations, coupled with elemental microanalysis, to examine iron sulfide growth textures and to establish whether early and late-forming CRMs involving greigite can be reliably distinguished.

SAMPLING AND METHODS

Standard paleomagnetic cores (25 mm diameter) were taken from the base of cliffs on Waihau Beach, 35 km northeast of Gisborne (178.2°E, 38.3°S), as part of a larger sampling program to investigate the tectonic evolution of the Hikurangi Margin. Samples ~1 km north of this locality were previously reported to have a reversed polarity magnetization with a small declination anomaly, indicating that this part of the margin has not undergone vertical-axis rotations (Thornley, 1996). Our sampling was along strike (beds measured at 194/23 W) and was thus at approximately the same stratigraphic level. The lithology consisted of massive gray mudstone with interbedded tuffaceous layers of variable thickness (to 30 cm). The rocks are early late Miocene (8.8–11.0 Ma) in age (Mazengarb and Speden, 2000).

We collected 42 cores over a total stratigraphic thickness of 7.8 m, including 2 tuff beds (Fig. 1A); weathered surficial material was removed from the outcrop prior to sampling. Cores were stored and transported to the laboratory in a mu-metal shield. Stepwise demagnetization of the samples was undertaken

*E-mail: cjr01@soc.soton.ac.uk.

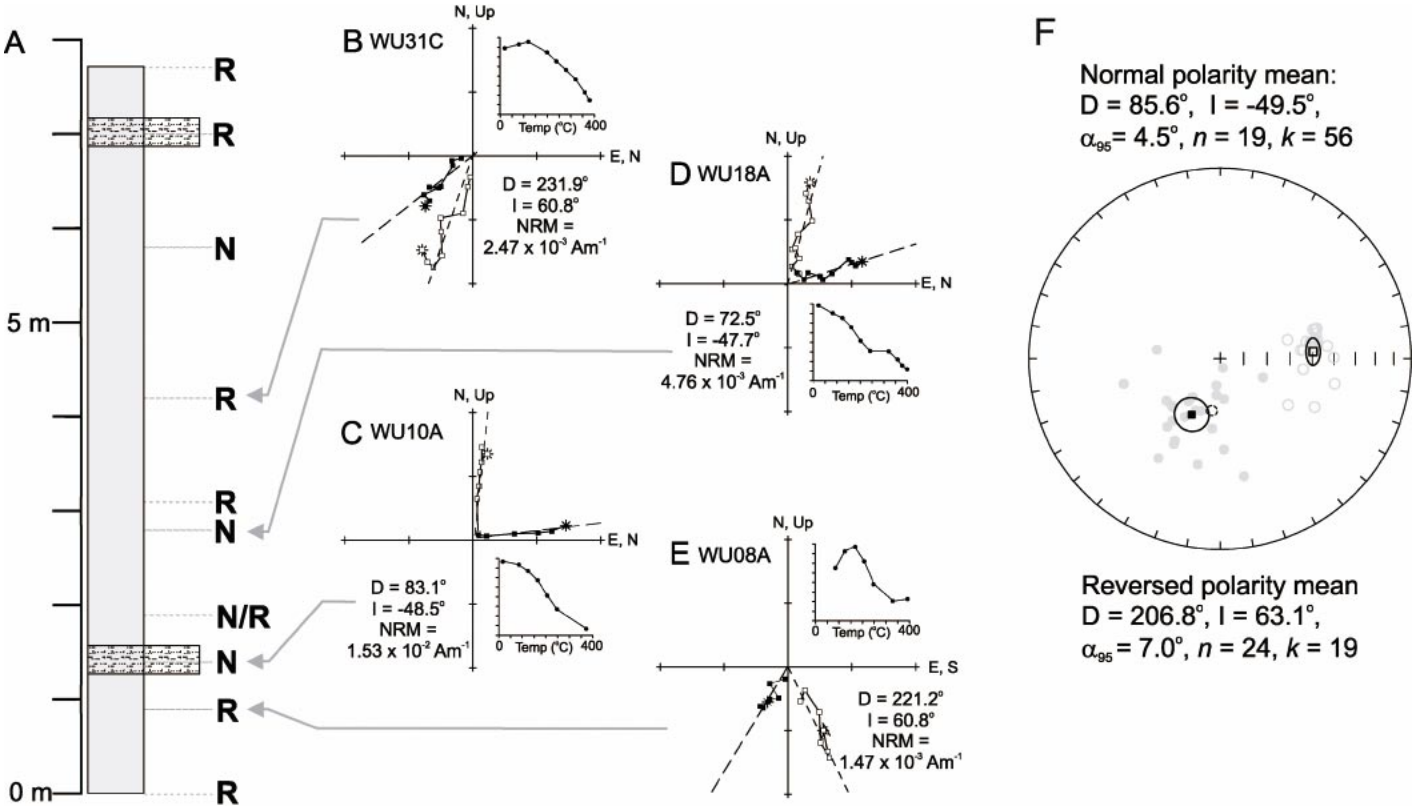

Figure 1. A: Stratigraphic column of sampled Waihau Beach locality, showing distribution of reversed (R) and normal (N) polarity remanent magnetizations through section. B–E: Representative vector demagnetization plots showing (C, D) normal polarity and large clockwise declination rotations and (B, E) reversed polarity and small rotations. Solid symbols denote declinations (D); open symbols denote inclinations (I). F: Equal-area stereographic plot of characteristic remanent magnetization directions in tilt-corrected coordinates, showing nonantipodal distribution of normal and reversed polarity directions. Mean direction of Thornley (1996) is plotted for comparison (small dashed error ellipse). NRM—natural remanent magnetization.

with a 2G-Enterprises cryogenic magnetometer in a magnetically shielded room at Southampton Oceanography Centre. Samples were demagnetized using both thermal (20°–60° steps to 400 °C) and alternating-field (5–10 mT steps to 60 mT) techniques. Where thermal demagnetization was used, low-field bulk magnetic susceptibility was measured after each heating step to monitor thermal alteration. Vector-component diagrams were used to identify samples where characteristic remanent magnetization (ChRM) directions could be isolated and analyzed using principal component analysis (Kirschvink, 1980).

Resin-impregnated polished sections were prepared for SEM analysis from paleomagnetic samples that had not been thermally demagnetized. Sedimentary microtextures were examined with a JEOL JSM-6360LV SEM operated at 15 keV with an 18 pA acceleration voltage at the Institute of Earth Sciences, Academia Sinica, Taipei, Taiwan. Mineral phases were identified with an Oxford Instruments Ltd INCA-300 energy dispersive spectrometer, with a pyrite (FeS_2) calibration standard. The high atomic mass of iron sulfides allows them to be easily identified by their high electron backscatter. It is possible to distinguish between greigite and pyrite from examination of the iron to sulfur ratio: Fe/S = 0.5 for pure pyrite, whereas for greigite, Fe/S = 0.75. Several studies have demonstrated that, with careful analysis, different sedimentary iron sulfides can be clearly distinguished (e.g., Jiang et al., 2001; Roberts and Weaver, 2005; Sagnotti et al., 2005). In this study the grain size of the iron sulfides being analyzed was often small with respect to the diameter of the electron beam (~1 μm), so elemental ratios reflected an average of several grains and the matrix between them. Careful examination was required to establish whether intermediate ratios ($0.5 \leq Fe/S \leq 0.75$) were due to a mixture of pyrite and greigite, rather than pyrite oxidation (which also leads to $Fe/S > 0.5$). Oxidation was inferred in analyses where large oxygen peaks occurred in the absence of silicate minerals.

RESULTS

The natural remanent magnetization (NRM) of the samples ranged from 1×10^{-4} to 2×10^{-2} Am^{-1}, although only the tuff samples had values exceeding 5×10^{-3} Am^{-1}. ChRMs were isolated from both thermally and alternating-field demagnetized samples, with the samples exhibiting unblocking temperatures of 280–380 °C and median destructive fields of 50–60 mT; thermal treatment generally yielded better-defined demagnetization trajectories. Both normal (Figs. 1C, 1D) and reversed (Figs. 1B, 1E) polarity directions were isolated; in all but one instance, polarities are consistent within a sampling level (Fig. 1A). In tilt-corrected coordinates, the normal-polarity samples give a mean direction of declination (D) = 85.6°, inclination (I) = −49.5°, α_{95} = 4.5°; the reversed-polarity samples give a mean direction of D = 206.8°, I = 63.1°, α_{95} = 7.0° (Fig. 1F). These directions are clearly not antipodal to one another, and the shallow dip of the beds means that they cannot be made so by unfolding (in geographic coordinates, the mean directions are D = 66.8°, I = −70.2° and D = 163.9°, I = 59.3°, respectively); nor do the normal-polarity directions result from a present-day overprint (D = 21°, I = −64°).

In the absence of local tectonic rotation, the expected declination for 10 Ma localities on the Australian plate is ~10°. The reversed-polarity direction has a declination of 27° ± 7°, which is close to that previously reported from nearby sediments (Thornley, 1996) (Fig.

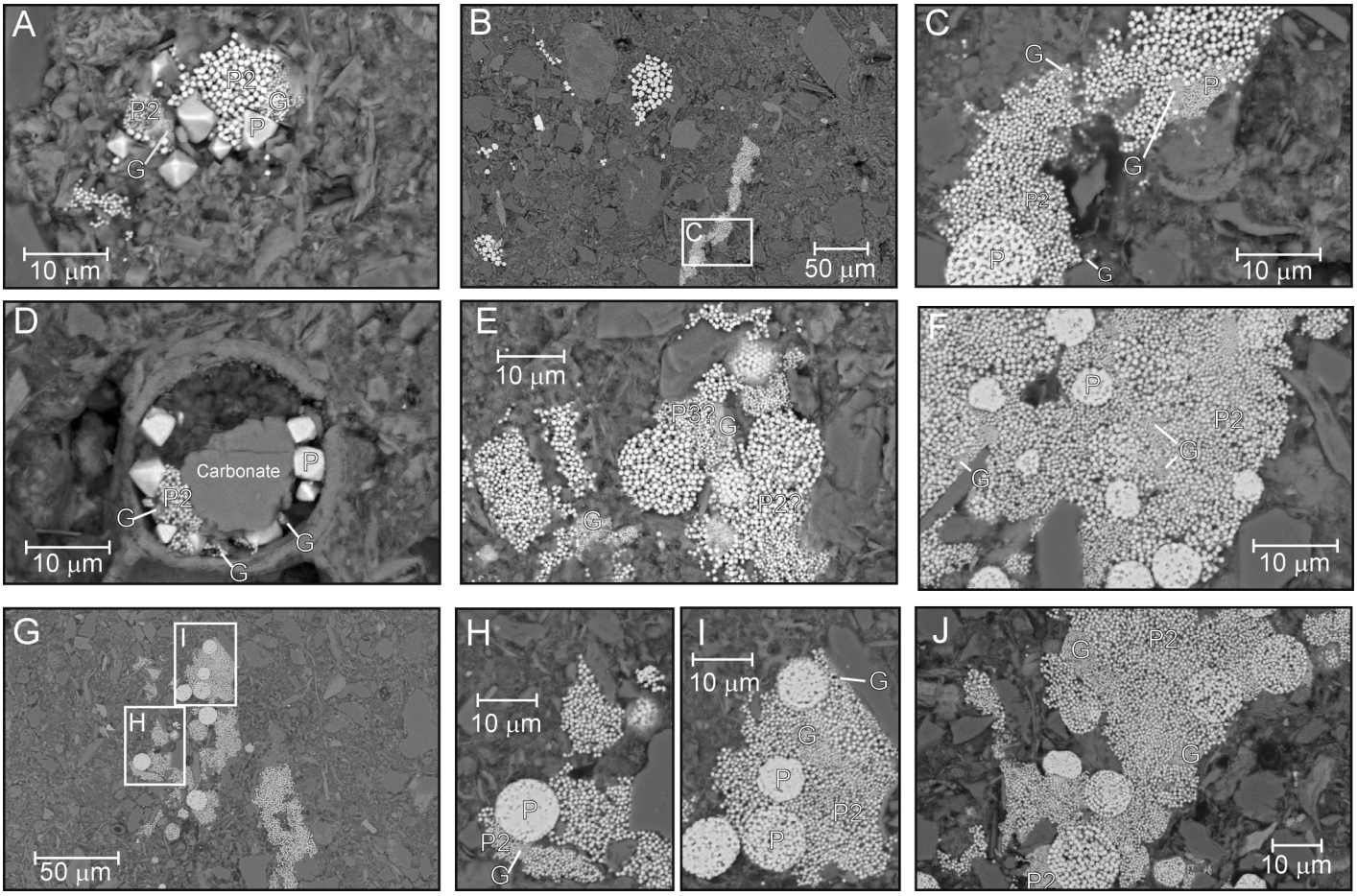

Figure 2. Backscattered electron images illustrating microtextures of several generations of authigenic greigite (G) and pyrite (P), from (A–E) sample with normal polarity, highly rotated, characteristic remanent magnetization direction, and (F–J) reversed polarity sample with small declination anomaly. A: Small iron sulfide aggregate consisting of early growth of euhedral pyrite P, followed by framboidal and space-filling pyrite P2 and neoformed greigite. B: Euhedral pyrite filling microfossils close to polyframboidal aggregate. C: Close-up view of aggregate in B. Neoformation of greigite is associated with space-filling P2 phase. D: Limited iron sulfide growth within a microfossil that has been partially infilled with carbonate cement. P2 pyrite and greigite have formed after euhedral pyrite (P). E: Close-up view of polyframboidal aggregate; different grain sizes possibly indicate two space-filling pyrite phases, tentatively labeled P2 and P3. Greigite neoformation is associated with these later phases. F: Close-up view of polyframboidal aggregate. First generation of framboidal pyrite (P) shows euhedral overgrowth. Isolated patches of greigite are surrounded by growth of pyrite P2. G: Polyframboidal aggregate. H: Close-up view of area indicated in G, showing greigite neoformation on surface of early framboid with euhedral overgrowth P, surrounded by space-filling pyrite (P2). I: Close-up view of area indicated in G. Greigite growth has occurred in a patch between recrystallized framboids (P), and on edge of a silicate grain, before growth of P2. J: Close-up view of polyframboidal aggregate; greigite has formed on edge of early framboids, and in isolated patches, before growth of space-filling pyrite phase (P2).

1F) and suggests minimal vertical-axis rotation. However, the large declination anomaly exhibited by the normal-polarity samples indicates substantial tectonic rotation. This discrepancy can be explained if the normal-polarity samples carry a magnetization that was acquired much earlier than that in the reversed-polarity samples, with a significant period of rotation in the interim.

Normal- and reversed-polarity samples were studied with the SEM; representative backscattered electron images are shown in Figure 2. Iron sulfides appear to be more abundant in the normal polarity samples, but are present throughout all the samples, studied, generally occurring in large aggregates representing several generations of iron sulfide growth, interpreted to represent progressively remineralized fragments of organic matter. In the normal-polarity samples, which document a large vertical-axis rotation, the first sulfide generation (marked P) consists of either euhedral pyrite crystals (Figs. 2A, 2D) or framboidal pyrite that often has euhedral overgrowths (Fig. 2C). Both forms can be observed in close proximity to each other (Fig. 2B), but their temporal relationship to each other is unclear. This first generation of iron sulfides is then surrounded by later growth of both greigite and at least one space-filling pyrite generation (P2); two phases of growth (P2 and P3) may be indicated by different grain sizes in the case of Figure 2E. Whereas in some cases greigite appears to postdate formation of P2 (Figs. 2A, 2E), in others the P2 phase has grown around the greigite (Fig. 2C). This suggests that the greigite and P2 formed penecontemporaneously; the greigite possibly formed as a precursor to P2, but in some places has been preserved, presumably due to incomplete pyritization.

In the reversed-polarity samples, which indicate minimal rotation, the first iron sulfide phase consists exclusively of framboidal pyrite, commonly with euhedral overgrowths (Figs. 2F, 2H, 2I). Greigite neoformation is observed at the edges of these framboids (Figs. 2H, 2J) and in isolated patches (Figs. 2F, 2I, 2J); in all cases this growth appears to have preceded a later space-filling generation of pyrite (P2, Figs. 2F, 2H–2J). In contrast to the paleomagnetic data, SEM observations indicate no clear differences in the mode of occurrence of remanence-bearing greigite in the

differently magnetized samples; in all cases it appears to have grown at an intermediate or late stage within authigenic iron sulfide aggregates that have undergone multiple generations of growth.

DISCUSSION AND CONCLUSIONS

Elemental analysis confirms the presence of authigenic greigite at the studied locality, in association with larger aggregations of authigenic iron sulfides. The demagnetization behavior of all samples is also consistent with the properties of greigite (Roberts, 1995; Sagnotti and Winkler, 1999), particularly the ~300–350 °C unblocking temperature, and higher coercivities than would be expected for magnetite. Additionally, the normal-polarity samples, which contain a greater abundance of iron sulfides, have higher NRM intensities (Figs. 2B–2E). These observations establish that greigite is the carrier of both the normal- and reversed-polarity magnetizations. No sample appears to contain both components; the formation of the later CRM appears to have destroyed or completely obscured the earlier remanence.

The magnetic properties and demagnetization behavior described here are also consistent with those reported from Cenozoic marine mudstones elsewhere in New Zealand (Turner, 2001, and references therein). These sediments have been through multiple episodes of uplift, erosion, redeposition, and reductive diagenesis, all of which have led to the dissolution of detrital magnetic minerals such as magnetite and growth of abundant pyrite. Greigite was documented in similar sediments in New Zealand by Roberts and Turner (1993), who concluded that it formed near the time of deposition rather than during later diagenesis. Our results indicate that this is not always the case. The presence of a remanent magnetization carried by a potentially late-forming authigenic mineral phase clearly has implications for the reliability of paleomagnetic studies in this region, and also in other regions with similar lithologies. For example, abundant greigite has been reported from Italian Neogene sequences (e.g., Sagnotti and Winkler, 1999), which also provide important midlatitude biostratigraphic zonations.

The locality reported here is important because a late remagnetization has only patchily overprinted an earlier CRM. In contrast to a similar case reported by Sagnotti et al. (2005), in which the early magnetization was carried by magnetite, here both early and late magnetizations are carried by greigite. The shallow tilt of the beds sampled means that the 60° differences in declination can only be due to several million years of vertical-axis rotation occurring between the times of acquisition of the two magnetizations. Samples showing both types of paleomagnetic behavior exhibit several generations of sulfide growth, with greigite forming at an intermediate to late stage. Thus, the relative timing of formation of the remanence-bearing phases appears to be similar, although the absolute timing clearly differs. It may therefore be difficult to discriminate between late and early magnetizations at sites where greigite is the dominant magnetic mineral. The section sampled by Thornley (1996), nearby on the same beach, records only the later magnetization reported here; as a result this area was mistakenly considered to be unaffected by Neogene tectonic rotations. Tectonic information has been lost in this case, and magnetostratigraphic data from these sediments would also be unreliable. Our results suggest that this is unlikely to be obvious from SEM observations.

If greigite is a common magnetic carrier in New Zealand Cenozoic mudstones, late-forming CRMs may potentially affect many of the data pertaining to the Neogene rotation of the Hikurangi Margin, as well as Cenozoic magnetostratigraphy. Any such studies should routinely incorporate petrographic observations to establish whether iron sulfides are present; in such cases, both in this region and in other regions where greigite is the dominant magnetic mineral, an early date for remanence acquisition should not be assumed in the absence of firm evidence, such as fold tests, reversals tests, or other field tests.

ACKNOWLEDGMENTS

This research was supported by contributions from the UK Natural Environmental Research Council (grant NER/S/2001/06363), the Leverhulme Trust, and the Royal Society of London. We thank Y. Iizuka and Y.H. Shau for invaluable assistance with scanning electron microscope analysis; John Geissman, Doug Elmore, and Gary Wilson for constructive reviews; and Hugh Jenkyns for editorial handling.

REFERENCES CITED

Beavan, J., and Haines, J., 2001, Contemporary horizontal velocity and strain rate fields of the Pacific-Australian plate boundary zone through New Zealand: Journal of Geophysical Research, v. 106, p. 741–770, doi: 10.1029/2000JB900302.

Berner, R.A., 1984, Sedimentary pyrite formation—An update: Geochimica et Cosmochimica Acta, v. 48, p. 605–615, doi: 10.1016/0016-7037(84)90089-9.

Florindo, F., and Sagnotti, L., 1995, Palaeomagnetism and rock magnetism in the upper Pliocene Valle Ricca (Rome, Italy) section: Geophysical Journal International, v. 123, p. 340–354.

Jiang, W.T., Horng, C.S., Roberts, A.P., and Peacor, D.R., 2001, Contradictory magnetic polarities in sediments and variable timing of neoformation of authigenic greigite: Earth and Planetary Science Letters, v. 193, p. 1–12, doi: 10.1016/S0012-821X(01)00497-6.

Kao, S.J., Horng, C.S., Roberts, A.P., and Liu, K.K., 2004, Carbon-sulfur-iron relationships in sedimentary rocks from southwestern Taiwan: Influence of geochemical environment on greigite and pyrrhotite formation: Chemical Geology, v. 203, p. 153–168, doi: 10.1016/j.chemgeo.2003.09.007.

Kirschvink, J.L., 1980, The least squares line and plane and the analysis of palaeomagnetic data: Royal Astronomical Society Geophysical Journal, v. 62, p. 699–710.

Mazengarb, C., and Speden, I.G., 2000, Geology of the Raukumara area: Lower Hutt, New Zealand, Institute of Geological and Nuclear Sciences Limited, Geological Map 6, scale 1:250,000.

Rait, G.J., Chanier, F., and Waters, D.W., 1991, Landward- and seaward-directed thrusting accompanying the onset of subduction beneath New Zealand: Geology, v. 19, p. 230–233, doi: 10.1130/0091-7613(1991)0192.3.CO;2.

Roberts, A.P., 1995, Magnetic properties of sedimentary greigite (Fe_3S_4): Earth and Planetary Science Letters, v. 134, p. 227–236.

Roberts, A.P., and Turner, G.M., 1993, Diagenetic formation of ferrimagnetic iron sulphide minerals in rapidly deposited marine sediments, South Island, New Zealand: Earth and Planetary Science Letters, v. 115, p. 257–273, doi: 10.1016/0012-821X(93)90226-Y.

Roberts, A.P., and Weaver, R., 2005, Multiple mechanisms of remagnetization involving sedimentary greigite (Fe_3S_4): Earth and Planetary Science Letters, doi: 10.1016/j.epsl.2004.11.024 (in press).

Sagnotti, L., and Winkler, A., 1999, Rock magnetism and palaeomagnetism of greigite-bearing mudstones in the Italian peninsula: Earth and Planetary Science Letters, v. 165, p. 67–80, doi: 10.1016/S0012-821X(98)00248-9.

Sagnotti, L., Roberts, A.P., Weaver, R., Verosub, K.L., Florindo, F., Pike, C.R., Clayton, T., and Wilson, G.S., 2005, Apparent magnetic polarity reversals due to remagnetization resulting from late diagenetic growth of greigite from siderite: Geophysical Journal International, v. 160, p. 89–100, doi: 10.1111/j.1365-246X.2005.02485.x.

Thornley, S., 1996, Neogene tectonics of Raukumara Peninsula, Northern Hikurangi Margin, New Zealand [Ph.D. thesis]: Wellington, Victoria University of Wellington, 291 p.

Turner, G.M., 2001, Toward an understanding of the multicomponent magnetization of uplifted marine sediments in New Zealand: Journal of Geophysical Research, v. 106, p. 6385–6397, doi: 10.1029/2000JB900406.

Walcott, R.I., 1989, Paleomagnetically observed rotations along the Hikurangi Margin of New Zealand, *in* Kissel, C., and Laj, C., eds., Paleomagnetic rotations and continental deformation: Dordrecht, Kluwer, p. 459–471.

Wilkin, R.T., and Barnes, H.L., 1997, Formation processes of framboidal pyrite: Geochimica et Cosmochimica Acta, v. 61, p. 323–339, doi: 10.1016/S0016-7037(96)003201.

Manuscript received 28 November 2004
Revised manuscript received 17 January 2005
Manuscript accepted 22 January 2005

Printed in USA